Research Square

Preprints are preliminary reports that have not undergone peer review.
They should not be considered conclusive, used to inform clinical practice,
or referenced by the media as validated information.

N,N’-Bis(5-phenyl-5-dibenzo[a,d]cycloheptenyl)hexane-1,6-diamine as a host compound for pyridine and the methylpyridine isomers: selectivities, crystal structures and thermal stabilities

Benita Barton

benita.barton@mandela.ac.za

Nelson Mandela University

Mino Caira

University of Cape Town

Jarryd Vorgers

Nelson Mandela University

Research Article

Keywords: Supramolecular, host–guest, pyridine, methylpyridine, separation, selectivity

Posted Date: November 23rd, 2026

DOI: https://doi.org/10.21203/rs.3.rs-11645573/v1

License: This work is licensed under a Creative Commons Attribution 4.0 International License.
Read Full License

Additional Declarations: No competing interests reported.

N,*N'*-Bis(5-phenyl-5-dibenzo[a,d]cycloheptenyl)hexane-1,6-diamine as a host compound for pyridine and the methylpyridine isomers: selectivities, crystal structures and thermal stabilities

Benita Barton,*[a] Mino R. Caira*[b] and Jarryd A. Vorgers*[a]

[a]Department of Chemistry, PO Box 77000, Nelson Mandela University, Gqeberha (Port Elizabeth), 6031, South Africa. E-mail: benita.barton@mandela.ac.za; s219615039@mandela.ac.za

[b]Department of Chemistry, University of Cape Town, Rondebosch 7701, South Africa. E-mail: mino.caira@uct.ac.za

Abstract

In this work, *N*,*N'*-bis(5-phenyl-5-dibenzo[a,d]cycloheptenyl)hexane-1,6-diamine (**H**) demonstrated the ability to include pyridine (PYR) and the methylpyridine (2MP, 3MP and 4MP) isomers in separate crystallisation experiments. When presented with equimolar mixed guest solutions, the host selectivity depended on the number and the nature of the other guests present in the solution. Notably, however, 2MP remained consistently disfavoured in all of these instances. It was, furthermore, shown that the binary guest solutions 50:50, 60:40 and 80:20 PYR/2MP, 20:80 and 40:60 3MP/PYR, and 50:50, 60:40 and 80:20 PYR/4MP may each be separated using **H** as the separatory agent: all of these experiments furnished extremely high selectivity coefficients. In each of these cases, PYR was the favoured guest solvent. SCXRD experiments revealed isostructural host arrangements in the complexes with MP, while this packing in the PYR complex was different. Moreover, the PYR guest molecules were accommodated in infinite undulating channels; the MPs, on the other hand, were located in isolated voids. It was suggested that the increased affinity of **H** for PYR was that only this guest interacted with the host molecule through a non-classical hydrogen bond, while the MPs did not. Also, PYR interacted with **H** by means of three C–H···π close contacts; in the other three complexes, the number of such interactions was either fewer or, indeed, absent. Finally, thermal analysis showed the PYR-containing complex to be significantly less stable than the complexes with MP, and these observations were possibly as a result of the guest accommodation type: PYR was found in endless channels while the MPs were located in discrete cavities.

Keywords

Supramolecular; host–guest; pyridine; methylpyridine; separation; selectivity

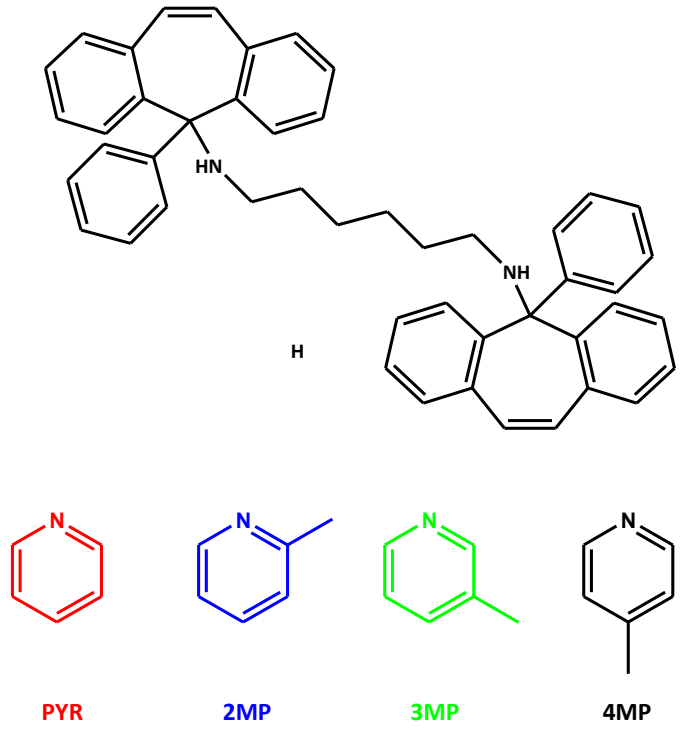
1. Introduction

Pyridine (PYR) and its three methylated positional isomers, 2-methylpyridine (2MP), 3-methylpyridine (3MP) and 4-methylpyridine (4MP) (Scheme 1), have wide-ranging and important applications in a number of different industries, including the chemical, biochemical and pharmaceutical sectors. PYR was first synthesized in 1876 from acetylene and hydrogen cyanide [1] while, historically, PYR and the MPs were extracted from coal tar but only in very modest quantities [2]. More recently, the production of these pyridines is readily achieved through the synthesis of aldehydes or ketones with ammonia, as reported by Chichibabin in 1924 [3,4], a method far superior to that contained in previous reports. As examples, acrolein and acetaldehyde react with ammonia to predominantly afford PYR, while acetaldehyde and ammonia undergo a gas-phase catalytic condensation reaction to produce 2MP and 4MP; a mixed product stream containing 3MP and PYR are, on the other hand, furnished upon reaction of acrolein alone with ammonia [5–7]. Therefore, in many instances, these synthetic routes result in mixtures of PYR and the MPs, and subsequent separation strategies are essential in order to

isolate each one with adequate purity for further applications [8]. To illustrate such applications, PYR functions primarily as a weakly basic, relatively unreactive solvent valued particularly in acylation and dehydrochlorination reactions in organic synthesis [9], and also serves as a solvent for paints, rubber processing, pharmaceutical manufacture, polycarbonate resin production, and water-repellent textile treatments [10]. The pyridyl derivatives are oftentimes responsible for the bioactivity that characterises many agricultural products, including herbicides, insecticides, fungicides, and plant growth regulators [4,9,10]. Moreover, 2MP serves as a precursor towards 2-vinylpyridine, which is required for the production of textile tyre chord, a terpolymer synthesised from each of 2-vinylpyridine, butadiene and styrene. Additionally, 2MP is employed in the preparation of several medications and agrochemicals, and examples include nitrapyrin, a preventative agent for ammonia loss from fertilisers, picloram, a herbicide, and amprolium, a coccidiostat [11]. 3MP, similarly, has a role to play in the agrochemical and pharmaceutical sectors. This compound is required for the preparation of the insecticide chlorpyrifos and the herbicide fluazifop-butyl, as well as the food additives nicotinic acid, nicotine carboxamide, niacin and its amide [12]. Finally, 4MP is primarily employed in the production of the antituberculosis agent isoniazid (isonicotinic hydrazide) and, moreover, serves as a precursor towards 4-vinylpyridine, a valuable monomer which is essential for the production of polymeric anion exchange resins and membranes [13].

Traditional industrial separations of PYR and the MPs principally rely on distillation techniques. However, these are extremely challenging owing to the comparable boiling points of, more especially, the MPs (2MP boils at 129 °C, 3MP at 144 °C and 4MP at 145 °C), resulting in complicated, costly and energy-intensive processes [14,15]. Other separation methods that have been investigated include, for example, dissociation extraction, but this too has its own limitations [16,17]. Consequently, the development of alternative, simple and energy-efficient strategies for such separations remains important. Over the past several decades, separation protocols of mixtures comprising compounds with similar boiling points based on host–guest chemistry have emerged as potential alternatives to tedious fractional distillations. As such, various host frameworks have been reported to possess selective recognition when presented with various mixed guest systems, including macrocyclic calixacridans, hybridarenes, cucurbiturils and resorcinarenes, and relatively smaller clathrand-type host species [18–23]. Our research group in particular has considered this latter category (clathrands) for the separations of isomers and related compounds, and applicable examples are those with the wheel-and-axle design [24–26], those possessing tricyclic fused moieties [27,28], various diols [29], compounds with a roof-shaped geometry [30], and molecules derived from tartaric acid [31].

In our quest to identify host compounds with enhanced preferential behaviours and with complementary selectivities relative to known reports, we considered *N*,*N*′-bis(5-phenyl-5-dibenzo[a,d]cycloheptenyl)hexane-1,6-diamine (**H**, Scheme 1) as a host candidate for the separation of mixed pyridines. The results of such an investigation have not been reported on any platform to date. The proposed study was deemed an appropriate one since related species *N*,*N*′-bis(5-phenyl-5-dibenzo[a,d]cycloheptenyl)ethylenediamine and *N*,*N*′-bis(5-phenyl-10,11-dihydro-5-dibenzo[a,d]cycloheptenyl)ethylenediamine demonstrated significantly enhanced affinities for 2MP and PYR, respectively [28], alluding to plausible separation protocols with these host candidates. Therefore, in the present work, **H** was subjected to a number of different crystallization experiments in order to ascertain its host ability for these pyridines and to determine whether separations of mixtures of these is reasonable by presenting **H** with a number of different guest solutions. Single crystal X-ray diffraction and thermal experiments were employed for the scrutiny of any complexes that formed successfully. This allowed the non-covalent interactions governing guest retention within the crystals to be identified as well as other relevant crystal structure parameters, together with the relative complex stabilities (determined from the onset temperature of guest release event, T_{on}). All results so obtained are provided herein.



Scheme 1 *N*,*N'*-Bis(5-phenyl-5-dibenzo[a,d]cycloheptenyl)hexane-1,6-diamine (**H**) and the four pyridyl guest species, pyridine (PYR) and 2-, 3- and 4-methylpyridine (2MP, 3MP and 4MP).

2. Experimental

2.1 General

The pyridyl solvents and the precursors required for the synthesis of **H** were procured from Merck, South Africa; these were used as obtained.

^{1}H-NMR experiments were carried out in $CDCl_3$ using a Bruker Ultrashield Plus 400 MHz NMR spectrometer; the data were analysed using TopSpin 4.2.0 software.

Intensity data were collected using a Bruker D8 VENTURE diffractometer with graphite-monochromated MoKα radiation (λ = 0.71073 Å). Crystals were mounted on nylon loops and cooled to 100(2) K using an Oxford Cryosystems Ltd. (Oxford, U.K.) cryostream with N_2 vapour. APEX3/v2019.1-0 (Bruker) software was used to control data collection [32]. Data reduction and unit cell refinement were performed with SAINT v8.40A (Bruker). Absorption corrections were applied using the multi-scan method in SADABS (2016/2) [33]. The structure was solved and refined via full-matrix least-squares using the SHELX suite [34], with X-Seed (Version 4.0) used as the graphical interface [35]. All non-hydrogen atoms were refined anisotropically. Once located, hydrogen atoms were mostly placed in idealised positions using a riding model, with U_{iso} values set between 1.2 and 1.5 times those of their respective parent atoms. The exception was the H atoms attached to nitrogen atoms exhibiting trigonal pyramidal geometry, which were refined freely. The crystal structures of **H**·2(PYR), **H**·0.5(2MP), **H**·0.5(3MP) and **H**·0.5(4MP) were deposited at the Cambridge Crystallographic Data Centre (CCDC), and their deposition numbers are 2536897, 2536898, 2536899 and 2536903, respectively.

Gas chromatographic (GC) analysis was carried out by means of an Agilent 7890A GC instrument coupled to a flame ionisation detector. The applicable stationary phase was an Agilent J&W Cyclosil-B capillary column. All samples, after isolation and washing with low boiling petroleum ether (b.p. 40–60 °C), were dissolved in dichloromethane prior to these analyses. The oven temperature program commenced at 50 °C, which was then

ramped up to 100 °C at a heating rate of 5 °C·min^{-1} and held at this temperature for 5 min. The carrier gas (He) flow rate was 1.5 mL·min^{-1} and the split ratio 1:80.

Thermal analyses were performed using a TA SDT Q600 module system. Complexes were isolated from their solutions by vacuum filtration, and the resulting crystals were washed (still under suction) with low boiling petroleum ether (b.p. 40–60 °C) before being patted dry in folded filter paper. The data obtained were analysed using PYRIS software. Samples were heated in ceramic pans, an empty pan serving as the reference, at a heating rate of 10 °C·min^{-1} from approximately 40 to 300 or 350 °C, under a purge gas of high purity nitrogen.

2.2 Synthesis of *N*,*N'*-bis(5-phenyl-5-dibenzo[a,d]cycloheptenyl)hexane-1,6-diamine (H)

The host compound (**H**) was synthesised according to a previous report [36].

2.3 Crystallization experiments of H from each of the pyridyl guest species

Crystallisation experiments were carried out, in glass vials, to assess the host ability of **H** towards each of the four potential pyridyl guest solvents. In each experiment, **H** (0.05 g, 0.08 mmol) was dissolved in an excess of the solvent, with mild heating applied to ensure complete dissolution of the host species. The vials were left open to the ambient conditions and, in such conditions, crystal growth was facilitated. The resulting crystals were isolated by vacuum filtration, washed with low boiling petroleum ether (b.p. 40–60 °C) and analysed using ^{1}H-NMR spectroscopy. Successful complexation was confirmed when both host and guest resonance signals appeared on the resultant spectra. The host:guest (H:G) ratio of each complex was then calculated by comparing the integrated areas of relevant host and guest resonance signals.

2.4 Host selectivity behaviour in mixed guest solutions

The preferential behaviour of **H** was investigated by means of two different experiments. In the first, **H** was crystallised from equimolar guest solutions and in the second, crystallisations were from binary guest mixtures containing different proportions of each guest solvent. More detail follows.

2.4.1 Crystallisation experiments of H from equimolar mixed pyridyls

The selectivity of **H** was then investigated through crystallisation experiments from equimolar mixed guest solutions, whilst considering all possible guest combinations. In these experiments, **H** (0.05 g, 0.08 mmol) was dissolved in the prepared equimolar guest mixtures (3–5 mmol combined amount) and the vials sealed and stored at the ambient conditions. The crystals that formed in this manner were isolated and analysed as described in the single guest experiments. GC analysis was employed to determine the relative guest amounts within each mixed guest complex, while ^{1}H-NMR spectroscopy was appropriate to establish the overall H:G ratios.

2.4.2 Crystallisation experiments of H from binary pyridyl guests in different molar ratios

The selectivity of **H** was, additionally, investigated when crystallised from binary guest solutions in which the proportions of the two guests present were varied sequentially. Therefore, **H** (0.05 g, 0.08 mmol) was dissolved in binary guest solutions (3–5 mmol combined amount) in which Guest A (G_A) and Guest B (G_B) were combined in 20:80, 40:60, 60:40 and 80:20 molar ratios. These crystallisations were carried out as before, and the isolated crystals were analysed, once more, by means of GC to obtain the guest composition in each complex. Selectivity profiles were then constructed by plotting Z_A (or Z_B), the mole fraction of G_A (or G_B) in the crystalline phase, against X_A (or X_B), the mole fraction of G_A (or G_B) in the original binary guest solution, as suggested by the equation of Pivovar *et al.*, $K = Z_B/Z_A \times X_A/X_B$, where $X_A + X_B = 1$ [37]. These plots visually represent the selectivity behaviour of **H** in such conditions. The selectivity coefficient (K) is a means of quantifying the host selectivity and may be calculated for each data point in these profiles. For meaningful separations of these binary mixtures through host–guest chemistry strategies, K is required to be 10 or greater [38,39]. On the other hand, when K = 1, the

host compound possesses no selectivity, which is represented by the diagonal line included in each profile so that ready comparisons may be made with the experimentally obtained data points.

2.5 Software

The crystal structures that were obtained from the SCXRD experiments were analysed by means of program Mercury [40], which was appropriate for the generation of unit cell diagrams, to demonstrate the packing within these, for illustrating the non-covalent interactions present, and to investigate the nature of the voids in which the guest molecules were located, whether in isolated cages or in infinite channels. In this case, the guest species were removed from the packing calculations which resulted in empty spaces, and these were analysed using a probe with a radius of 1.2 Å.

3. Results and discussion

3.1 Crystallization experiments of H from each of the pyridyl guest species

Host crystallization experiments from each of these pyridines afforded inclusion complexes in each instance, as determined through ^{1}H-NMR analysis. The H:G ratio of the complex with PYR was 2:3, while each of the methylpyridines was enclathrated with 2:1 H:G ratios (Table 1). (The applicable ^{1}H-NMR spectra are provided in the Supplementary Information section.)

Table 1 Complexes of **H** when crystallised from each of the pyridines.

Guest solvent	H:G ratio
PYR	2:3
2MP	2:1
3MP	2:1
4MP	2:1

3.2 Host selectivity behaviour in mixed guest solutions

Since **H** possessed inclusion ability for each of the four pyridyls, its selectivity behaviour in mixed guest solutions was subsequently investigated, in both equimolar guest and in non-equimolar binary guest solutions.

3.2.1 Crystallisation experiments of H from equimolar mixed pyridyls

Table 2 contains a summary of the results obtained when **H** was crystallised from all combinations of equimolar guest mixtures. It was deemed pertinent to carry out each experiment in duplicate so that the repeatability of the results could be determined. As such, also provided in each instance is the percentage estimated standard deviation (% e.s.d.). For facile scrutiny, favoured guests are highlighted in this table by means of bold red text.

Table 2 The guest and overall H:G ratios of complexes formed in the equimolar guest mixtures.[a]

PYR	2MP	3MP	4MP	G:G	Overall H:G ratio	% e.s.d.
X	X			**100.0**:0.0	2:1	0.0
X		**X**		13.8:**86.2**	2:1	1.2
X			X	**100.0**:0.0	1:1	0.0
	X	**X**		26.3:**73.7**	2:1	0.6
	X		**X**	24.4:**75.6**	2:1	0.8
		X	**X**	38.2:**61.8**	1:1	1.1
X	X	**X**		8.7:22.3:**69.0**	2:1	1.1:2.9:4.1
X	X		**X**	6.3:20.9:**72.8**	2:1	1.3:1.1:0.1
X		X	X	**100.0**:0.0:0.0	1:1	0.0
	X	X	**X**	13.5:35.1:**51.4**	2:1	2.6:2.3:0.0
X	X	X	**X**	4.7:13.5:33.0:**48.8**	2:1	0.5:2.3:0.3:3.1

The results in Table 2 indicate that each of PYR, 3MP and 4MP were preferred by **H** depending on which guest solvents were present in the solution. Contrarily, 2MP was unfailingly disfavoured in all of these experiments. Remarkably, the PYR/2MP and PYR/4MP binary solutions furnished crystals that contained only PYR (100.0%), while the solids isolated from the 2MP/4MP and 3MP/4MP mixtures contained enhanced amounts of 4MP (75.6% and 61.8%, respectively). In the absence of both PYR and 4MP (2MP/3MP), more of 3MP was selected, and 73.7% of this guest solvent was measured in the crystals. Interestingly, and contrary to prediction, **H** selected more of 3MP (86.2%) when mixed equimolarly with PYR and, despite this not being an anticipated result, the % e.s.d. for this set of experiments was low (1.2%, Table 2), implying its replicability. As a plausible explanation for this apparent outlier, it must be borne in mind that, as an example, guests in the PYR/2MP experiment are not the same as in PYR/3MP (the environment in which the host compound finds itself is not comparable) and, as such, it is not surprising that predictions in these guest competition experiments are not always realised. (See also Figure 1b, later, where this unexpected result fits the profile for the PYR/3MP binary solution experiments.) A consideration of the results from the ternary experiments revealed that **H** selected only PYR (100.0%) in the PYR/3MP/4MP solution, a noteworthy finding given that three guest species in this instance competed for the voids in the complex, with only one succeeding to be accommodated. The PYR/2MP/4MP and 2MP/3MP/4MP solutions, on the other hand, produced crystals enriched in 4MP (72.8% and 51.4%), which was also the case when all four guest solvents were present (48.8% 4MP). Again, one “outlier” result was noted, that from the PYR/2MP/3MP experiment, in which more of 3MP (69.0%) was measured in the crystals compared with PYR (8.7%). Once more, a possible explanation for this observation is as provided for the PYR/3MP result discussed earlier. Finally, the overall H:G ratios were either 2:1 or 1:1, depending on the guest combination.

3.2.2 Crystallisation experiments of H from binary pyridyl guests in different molar ratios

Figures 1a–f illustrate the selectivity profiles of **H** when crystallised from PYR/2MP, 3MP/PYR, PYR/4MP, 3MP/2MP, 4MP/2MP and 4MP/3MP binary solutions containing varying guest proportions. For completeness, the equimolar binary mixed guest results (Table 2) have been inserted into these profiles also. The corresponding selectivity coefficients (K), determined for each data point, are summarised in Table 3, with those 10 or greater highlighted in bold red text signifying plausible separations through host–guest chemistry with **H** as the host candidate.

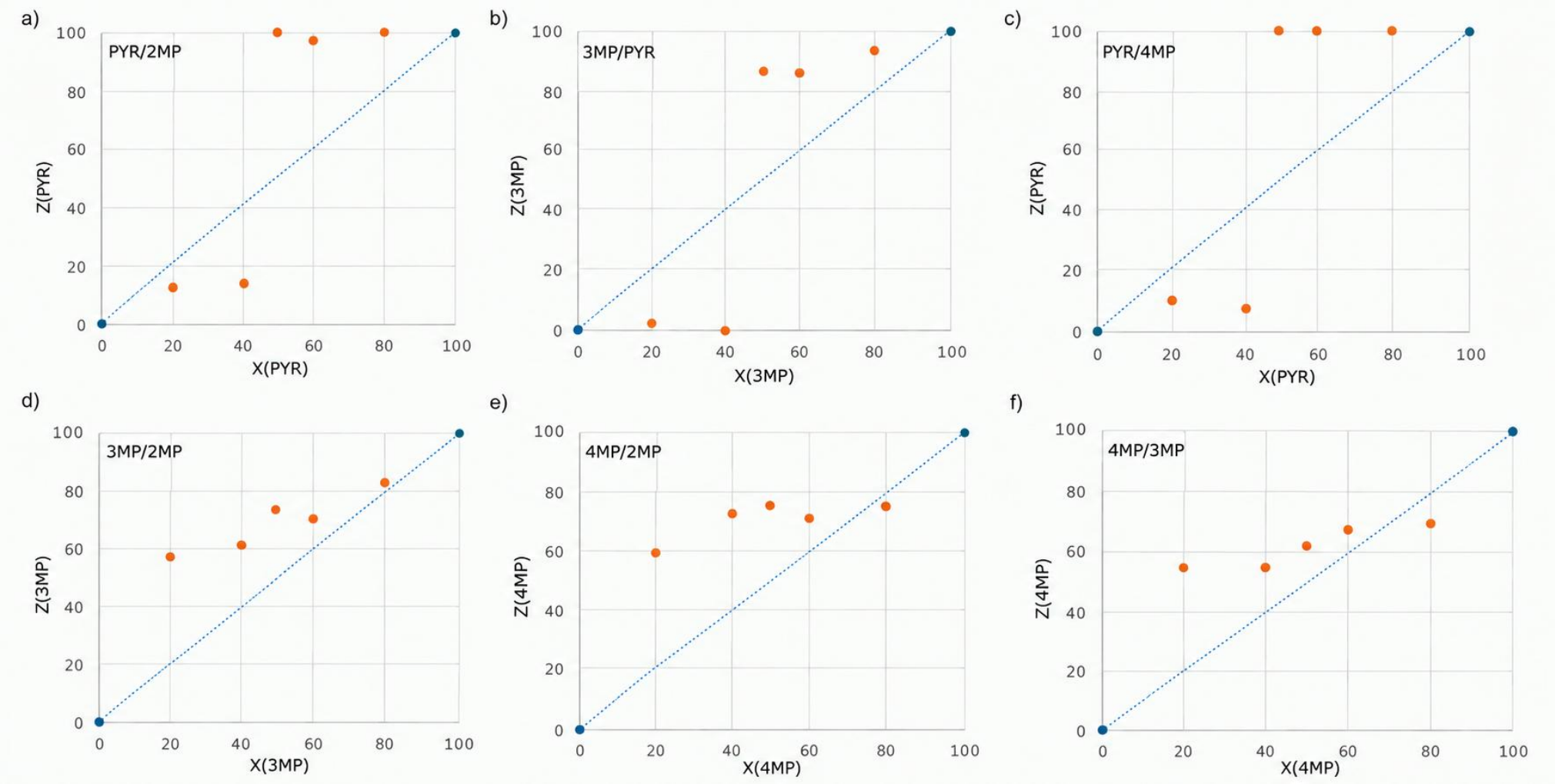


Figure 1 Selectivity profiles obtained for **H** when crystallised from the (a) PYR/2MP, (b) 3MP/PYR, (c) PYR/4MP, (d) 3MP/2MP, (e) 4MP/2MP and (f) 4MP/3MP binary solutions, with the inserted diagonal straight lines representing a host compound with no selectivity (K = 1).

Table 3 Calculated K values for **H** in the binary pyridyl solutions.

	K value (in favour of)				
Binary mixture	20:80	40:60	50:50	60:40	80:20
PYR/2MP	1.7 (2MP)	4.4 (2MP)	**∞ (PYR)**	**21.2 (PYR)**	**∞ (PYR)**
3MP/PYR	**12.5 (PYR)**	**∞ (PYR)**	6.2 (3MP)	4.0 (3MP)	3.8 (3MP)
PYR/4MP	2.6 (4MP)	8.4 (4MP)	**∞ (PYR)**	**∞ (PYR)**	**∞ (PYR)**
3MP/2MP	5.5 (3MP)	2.5 (3MP)	2.8 (3MP)	1.6 (3MP)	1.2 (3MP)
4MP/2MP	6.0 (4MP)	4.2 (4MP)	3.1 (4MP)	1.7 (4MP)	1.2 (2MP)
4MP/3MP	4.8 (4MP)	1.8 (4MP)	1.6 (4MP)	1.4 (4MP)	1.7 (3MP)

From Figure 2a (PYR/2MP), the host selectivity adjusted with guest concentration changes. At low concentrations of PYR (20:80 and 40:60), 2MP was favoured, while an increase in the amount of PYR (50:50, 60:40 and 80:20) resulted in **H** selecting more of PYR. The selectivity coefficients (K) when 2MP was preferred were low (1.7 and 4.4, Table 3), suggesting that **H** does not possess the ability to separate these two solutions (K is required to be 10 or greater). However, remarkable K values were calculated in the final three experiments which favoured PYR, ∞, 21.2 and ∞, respectively, and it is thus plausible that these solutions may be separated in this particular fashion.

Figure 2b (3MP/PYR) demonstrates, once more, a host selectivity that was guest concentration dependent. Low concentrations of 3MP (20:80 and 40:60) facilitated the enclathration of more of PYR, and the K values associated with these experiments were significant, 12.5 and ∞ (Table 3), and separations are feasible. However, the remaining three experiments, which favoured 3MP, furnished K values too low (3.8–6.2) to suggest that **H** would be able to separate these solutions.

When PYR and 4MP competed (Figure 2c), again, the affinity behaviour of **H** changed with guest concentration variances. The 20:80 and 40:60 PYR/4MP experiments produced crystals that were enriched in 4MP, but the K values were only modest (2.6 and 8.4). Remarkably, though, in the remaining three experiments (50:50, 60:40 and 80:20), only PYR was observed in the crystals and K was infinite; **H** would thus be extremely efficient for the separation of these three binary solutions.

The 3MP/2MP experiments (Figure 2d) demonstrated that 3MP was consistently selected for across the entire concentration range, but K was calculated to be between only 1.2 and 5.5, and the host species would not be effective in the separation of any of these mixtures.

From Figure 2e (4MP/2MP), only the 80:20 experiment resulted in a host selectivity for 2MP, while the remaining four experiments illustrated a consistent preference for 4MP. In all instances, K was insignificant, ranging between 1.2 and 6.0; no separations would, therefore, be plausible with **H** as the host species.

The results obtained in the 4MP/3MP experiments (Figure 2f) were comparable to those from the 4MP/2MP experiments (Figure 2e). Again, in only the 80:20 solution was the one guest, 3MP in this instance, preferred, while the other four experiments revealed a consistent preference for 4MP. Once more, K was low in each case, ranging between only 1.4 and 4.8; again, **H** would not serve as an effective separatory agent for any of these binary solutions.

In summary, the results emanating from these binary solution experiments suggest that each of the 50:50, 60:40 and 80:20 PYR/2MP, 20:80 and 40:60 3MP/PYR, and 50:50, 60:40 and 80:20 PYR/4MP mixtures may be separated/purified by means of **H** using host–guest chemistry, with more of PYR being extracted in each occurrence.

3.3 Single crystal X-ray diffraction experiments

Table 4 contains a summary of the relevant crystallographic parameters for obtaining the crystal structures of the four clathrates applicable to the present investigation. Each one crystallised in the triclinic crystal system and

space group *P*–1. The crystals selected for these analyses demonstrated H:G ratios of 1:2 for the PYR-containing complex and 1:0.5 for each of the MP inclusion compounds. Additionally, the host packing in **H**·2(PYR) was unique compared with the three MP complexes, the host assembly in these three being isostructural. The host molecule in **H**·2(PYR), furthermore, was situated on a centre of inversion, and its centrosymmetric conformation also differed from this molecule in the complexes with the MPs, where the host molecules were not located on centres of inversion and adopted a different, common conformation from the centrosymmetric one of **H**·2(PYR). Note that the H:G ratio of the crystal containing PYR selected for SCXRD analysis differed somewhat (1:2) from that obtained from ^{1}H-NMR spectroscopy (2:3). One plausible reason for this observation is that this complex was unstable at ambient conditions and, during preparation of the NMR sample, some guest evaporated from the crystal resulting in the 2:3 H:G measurement rather than the 1:2 observed from SCXRD analysis. This instability was confirmed later through thermal analysis (see the following section).

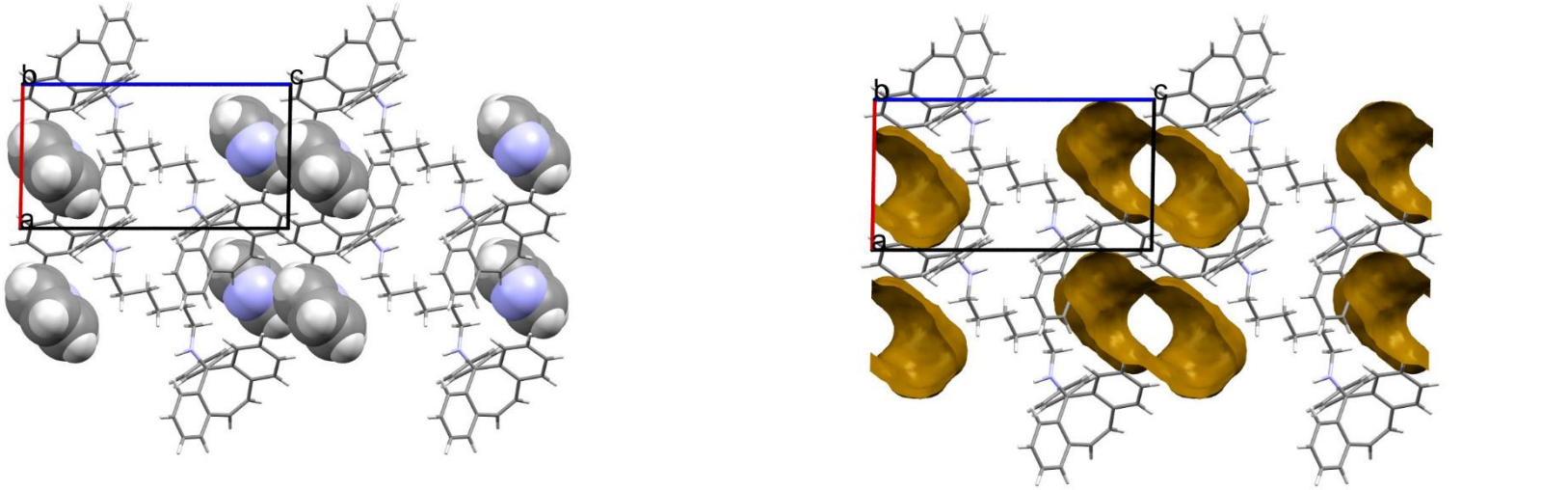
While the PYR guest molecule was ordered in its complex with **H**, in each of the three cases with the MPs, the guest species displayed disorder around a common centre of inversion. Moreover, the host molecule was ordered in **H**·0.5(3MP) and **H**·0.5(4MP), but in **H**·0.5(2MP), the host species demonstrated some disorder, and the appearance of two distinct –$(CH_2)_6$– components were observed, which were appropriately modelled, and the major component had a site occupancy factor (s.o.f.) of 0.590(4).

Figures 2a–d depict the unit cells and host–guest packing (left) and the calculated voids (right) for each of the four structures. The common host packing in the MP complexes is tangible when considering Figures 2b–d, this being considerably different from that in **H**·2(PYR). Furthermore, the PYR guest molecules were observed to occupy infinite and undulating channels (parallel to the b-axis) in the crystal of its complex while, contrastingly, the MP guest species were located in isolated cages in the centres of their respective unit cells.

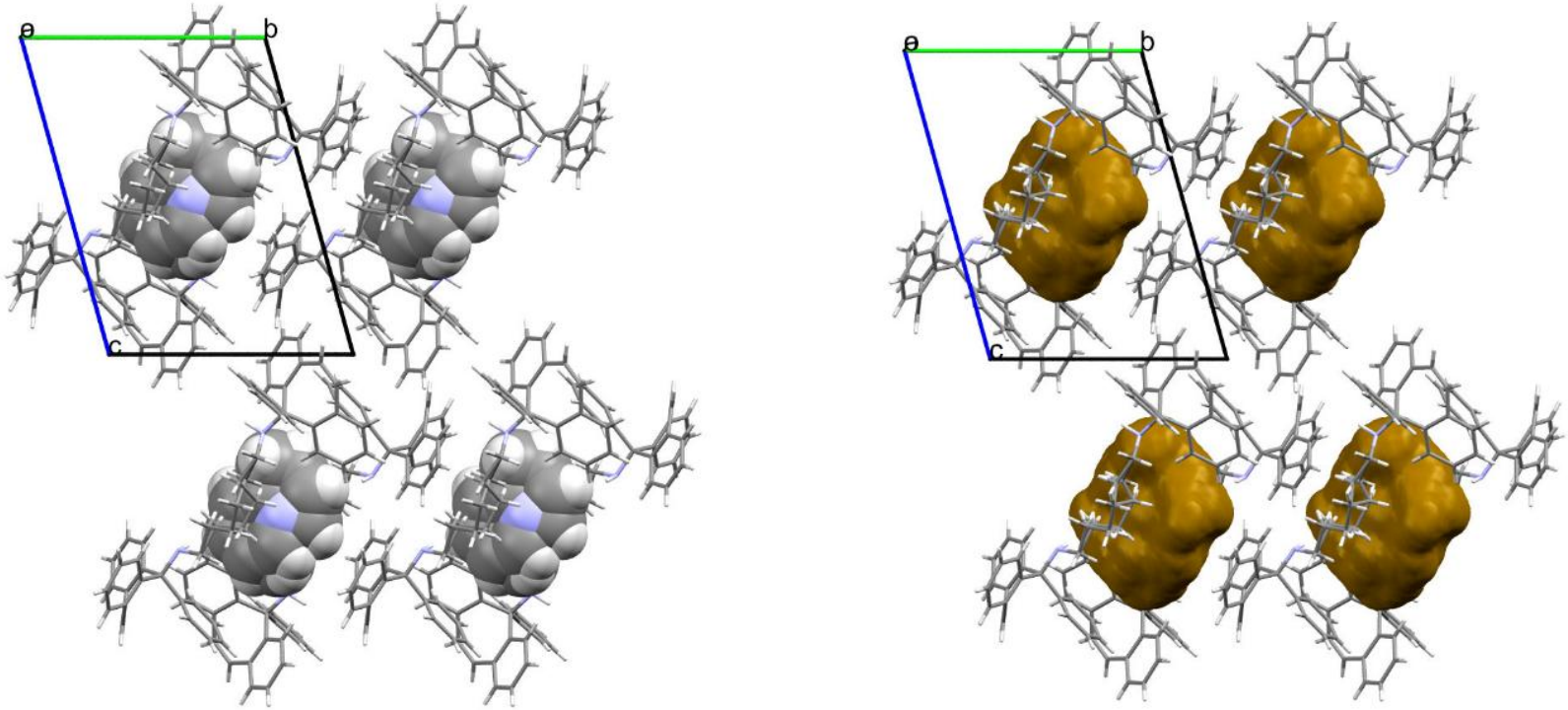
Table 4 Crystallographic data for the complexes of **H** with the four pyridyl guests.

	H·2(PYR)	**H**·0.5(2MP)	**H**·0.5(3MP)	**H**·0.5(4MP)
Chemical formula	$C_{48}H_{44}N_2 \cdot 2(C_5H_5N)$	$C_{48}H_{44}N_2 \cdot 0.5(C_6H_7N)$	$C_{48}H_{44}N_2 \cdot 0.5(C_6H_7N$)	$C_{48}H_{44}N_2 \cdot 0.5(C_6H_7N)$
Formula weight	807.05	695.41	695.41	695.41
Crystal system	triclinic	triclinic	triclinic	triclinic
Space group	*P*–1	*P*–1	*P*–1	*P*–1
μ (Mo-Kα)/mm^{-1}	0.072	0.071	0.070	0.071
a/Å	8.8720(4)	10.6950(17)	10.6525(4)	10.7465(4)
b/Å	8.9854(4)	12.664(2)	12.7484(5)	12.5855(6)
c/Å	15.0683(8)	15.738(2)	15.7164(6)	15.6725(7)
alpha/°	82.863(2)	74.483(5)	75.300(1)	71.925(1)
beta/°	87.882(2)	86.878(5)	87.085(1)	85.764(1)
gamma/°	64.809(2)	66.884(5)	66.646(1)	68.526(1)
V/Å^3	1078.39(9)	1886.0(5)	1892.35(13)	1873.33(14)
Z	1	2	2	2
F(000)	430	742	742	742
Temp./K	100	100	100	100
Restraints	0	0	10	7
Nref	5273	9392	9850	8638
Npar	285	560	523	521
R	0.0485	0.0508	0.0457	0.0485
wR2	0.0980	0.1209	0.1021	0.1006
S	1.05	1.02	1.02	1.03
θmin–max/°	2.5, 28.1	1.9, 28.4	2.0, 28.8	2.0, 27.6
Tot. data	36778	68642	97932	72804
Unique data	5273	9392	9850	8638
Observed data [I > 2.0 sigma(I)]	4565	7266	7547	6222
R_{int}	0.046	0.055	0.074	0.083
Completeness	0.998	0.999	0.998	0.999
Min. resd. dens./e·Å^{-3}	–0.22	–0.30	–0.23	–0.28
Max. resd. dens./e·Å^{-3}	0.26	0.81	0.34	0.32
Density/g·cm^{-3}	1.243	1.225	1.220	1.233
CCDC deposition numbers	2536897	2536898	2536899	2536903

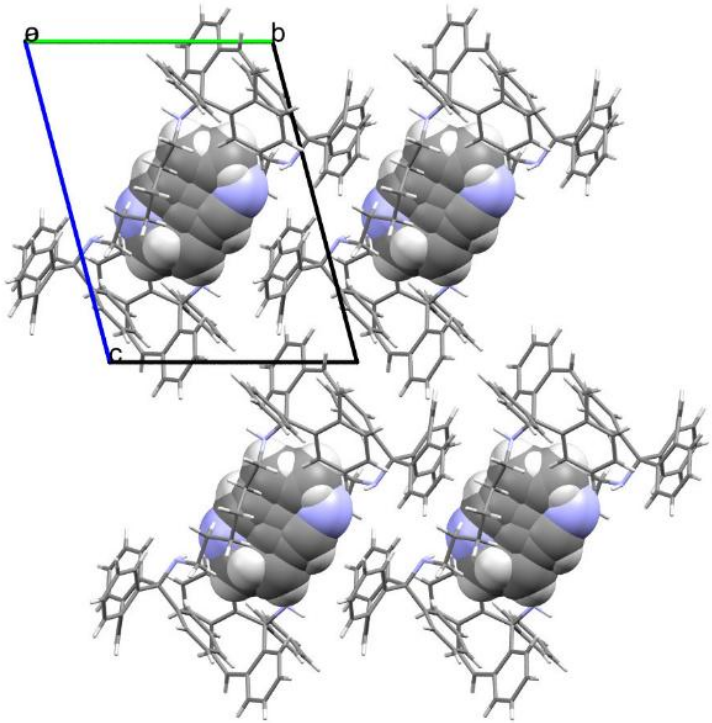
a)

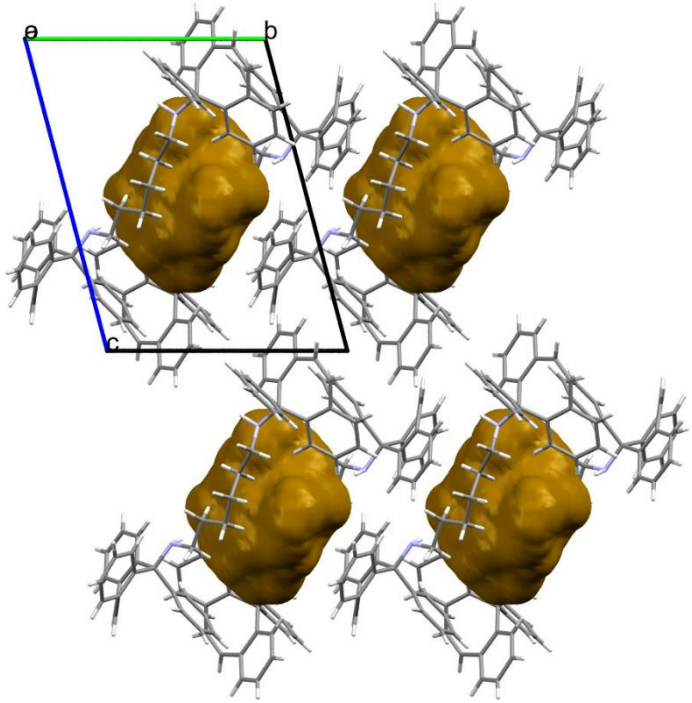


b)



c)





d)

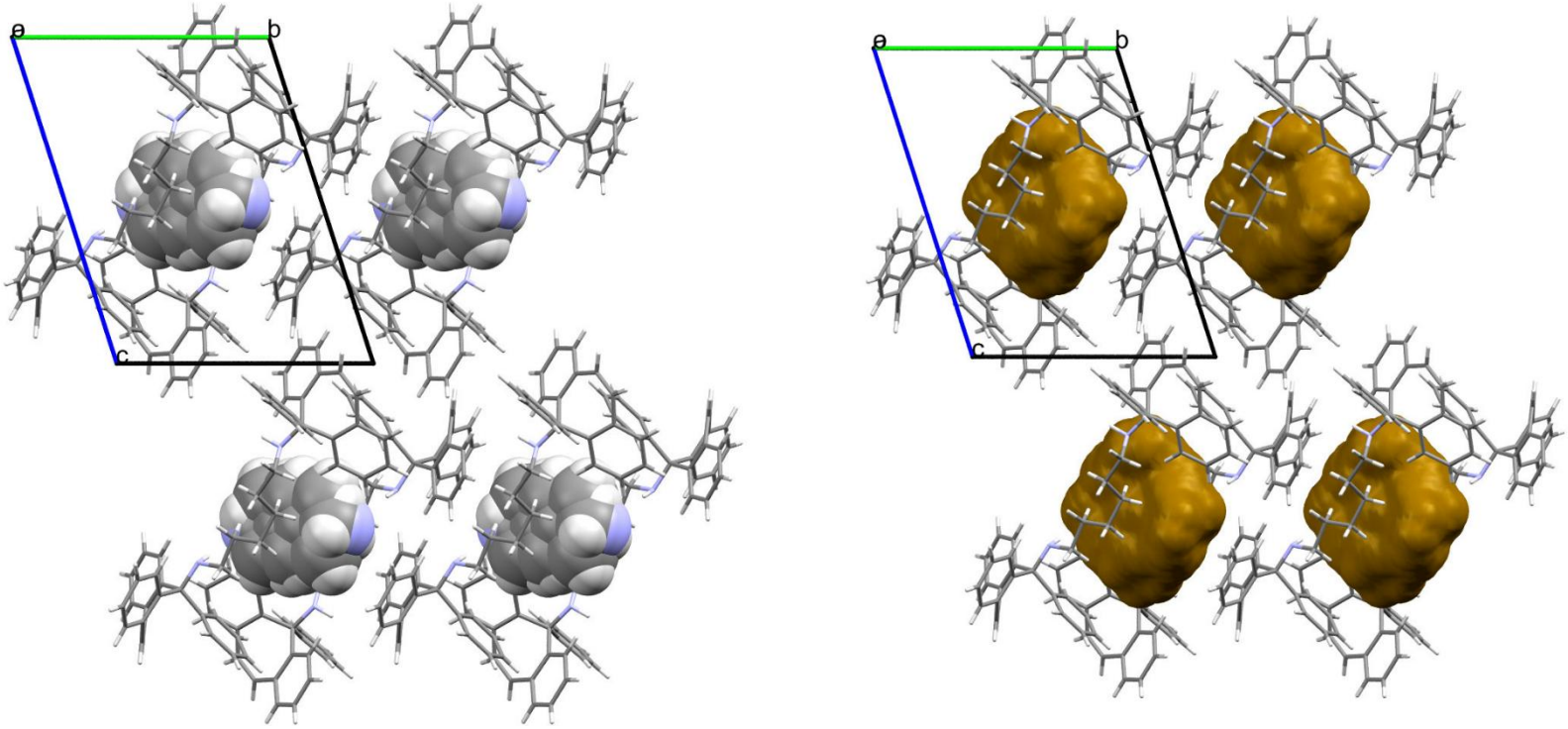


Figure 2 Unit cells and host–guest packing (left) and the corresponding void diagrams (right) for the complexes (a) **H**·2(PYR), (b) **H**·0.5(2MP), (c) **H**·0.5(3MP) and (d) **H**·0.5(4MP); host molecules are in capped stick and guests in spacefill representation.

A scrutiny of the non-covalent interactions present in each complex was subsequently undertaken. Surprisingly, owing to the myriad aromatic moieties present in each one, no significant π···π interactions could be identified.

In **H**·2(PYR), the guest molecule was retained in the complex through a (host)C–H···π(guest) close contact (Figure 3) which measured 2.96 Å (H···π) and 3.647(2) Å (C···π) (130°) and which involved a host aromatic proton. Also observed were two such interactions but with a host aromatic moiety serving as the centre of gravity ((guest)C–H···π(host)) (Figure 4), and applicable parameters were 2.86 and 2.88 Å, and 3.440(2) and 3.763(2) Å; the corresponding angles were 120 and 155°. No classical hydrogen bonds were present in this complex. Evident were, however, non-classical bonds of this type, one between the host and guest molecules (Figure 5), and two intramolecular within the host species. The former ((host)C–H···N(guest)) measured 2.50 Å (H···N) and 3.271(2) Å (C···N) (139°), while applicable parameters for those intramolecular in nature were 2.38 and 2.38 Å, and 2.762(2) and 2.765(2) Å (both angles being 104°).

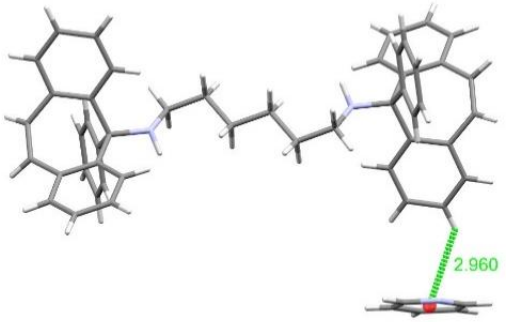


Figure 3 The (host)C–H···π(guest) interaction in **H**·2(PYR) (2.96 Å).

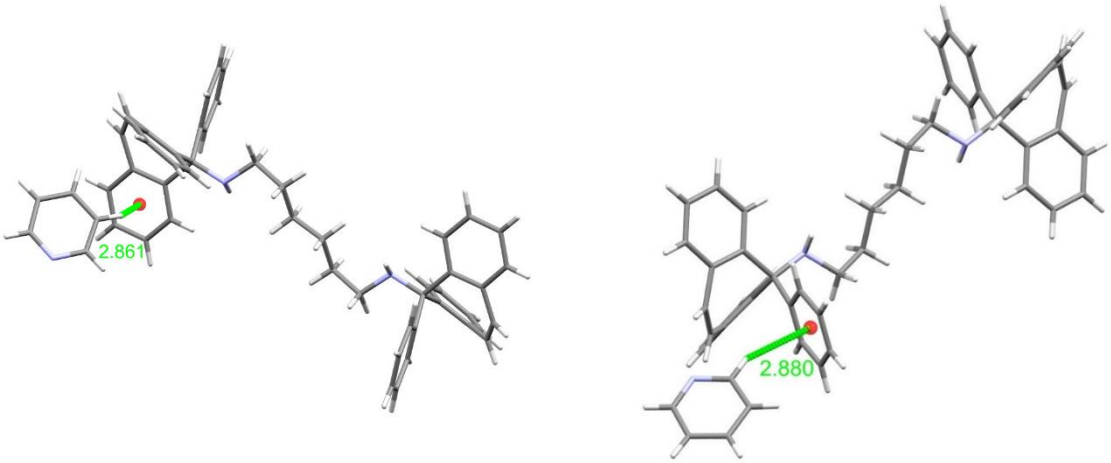


Figure 4 Two significant (guest)C–H···π(host) interactions in **H**·2(PYR) (2.86 and 2.88 Å).

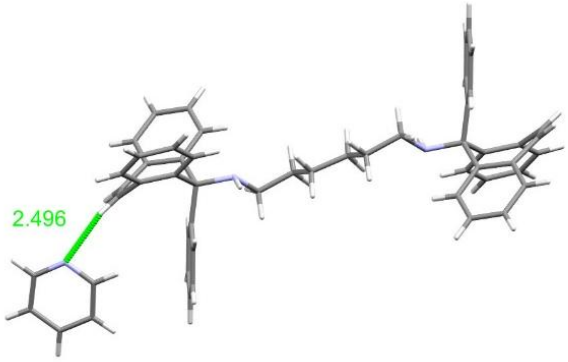


Figure 5 The non-classical (host)C–H···N(guest) hydrogen bonding interaction in **H**·2(PYR) (2.50 Å).

In the **H**·0.5(2MP) complex, the centre of gravity of the guest species interacted favourably with hydrogen atoms on the linker chain of the host molecule. Two such (host)C–H···π(guest) close contacts were identified. The applicable parameters were 2.52 and 2.93 Å, and 3.296(6) and 3.434(5) Å, with angles 135 and 112° (Figure 6). There were also no classical hydrogen bonds in this complex, as was the case in the PYR-containing inclusion compound. However, while PYR was engaged in a (host)C–H···N(guest) close contact with **H**, 2MP did not interact with the host molecule in this manner. It was observed that the host molecular geometry was stabilised through four intramolecular non-classical C–H···N hydrogen bonds with parameters 2.36–2.39 Å, 2.743(2)–2.764(2) Å and 103–104°.

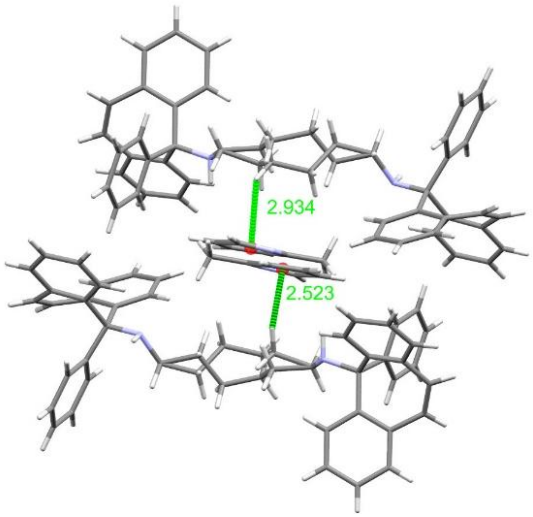


Figure 6 The two (host)C–H···π(guest) interactions in **H**·0.5(2MP) (2.52 and 2.93 Å).

The **H**·0.5(3MP) complex was, surprisingly, wholly devoid of any close contacts between the host and guest species, and guest retention must therefore have been as a result of steric factors alone. However, the usual intramolecular non-classical C–H···N hydrogen bonds within each host molecule, numbering four again, were identified (2.35–2.39 Å, 2.737(2)–2.767(2) Å and 103–104°) and facilitated in maintaining the geometry of the host molecule.

Finally, in the **H**·0.5(4MP) complex, one (host)C–H···π(guest) interaction was identified, measuring 2.84 Å, 3.639(4) Å and 138° (Figure 7). No other close contacts between the host and guest species were responsible for guest retention. Once more, four non-classical intramolecular host C–H···N hydrogen bonding interactions were also noted (2.36–2.41 Å, 2.745(2)–2.776(2) Å and 103–104°).

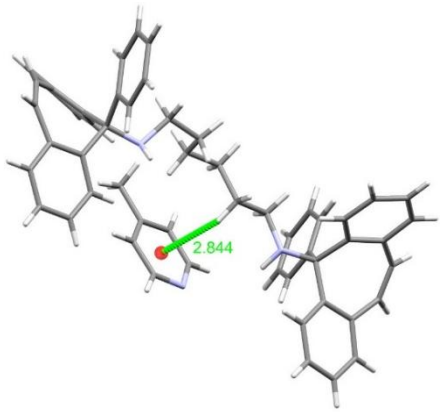


Figure 7 The (host)C–H···π(guest) interaction (2.84 Å) in **H**·0.5(4MP), the only close contact responsible for guest retention.

From this analysis of the close contacts present between the host and guest species, it is not immediately evident why 2MP was constantly disfavoured in the guest competition experiments (Table 2). Two (host)C–H···π(guest)

interactions were observed in its complex, while no host···guest interactions were present in **H**·0.5(3MP), and yet it was a preferred guest solvent on a number of occasions. Additionally, **H**·0.5(4MP) experienced only one interaction of this type, but it was favoured in several of the competition experiments. However, these SCXRD analyses do explain the enhanced selectivity of **H** for PYR (Table 3): aside from the three C–H···π interactions (a greater number than in any of the other complexes) observed in the PYR-containing inclusion compound, PYR was the only guest species of the four to interact with **H** by means of a non-classical (host)C–H···N(guest) hydrogen bond.

3.4 Thermal analyses

The four complexes were subsequently subjected to a controlled heating program through thermal analysis by employing a heating rate of 10 °C·min^{-1}. The resulting thermograms are presented in Figures 8a–d, and the corresponding data from these are summarised in Table 5. Here, T_{on} denotes the onset temperature of the guest release event and serves as an indicator of the relative thermal stability of each complex, while T_p is the endotherm peak temperature, obtained from the DSC curve, representing the point of most rapid host melting.

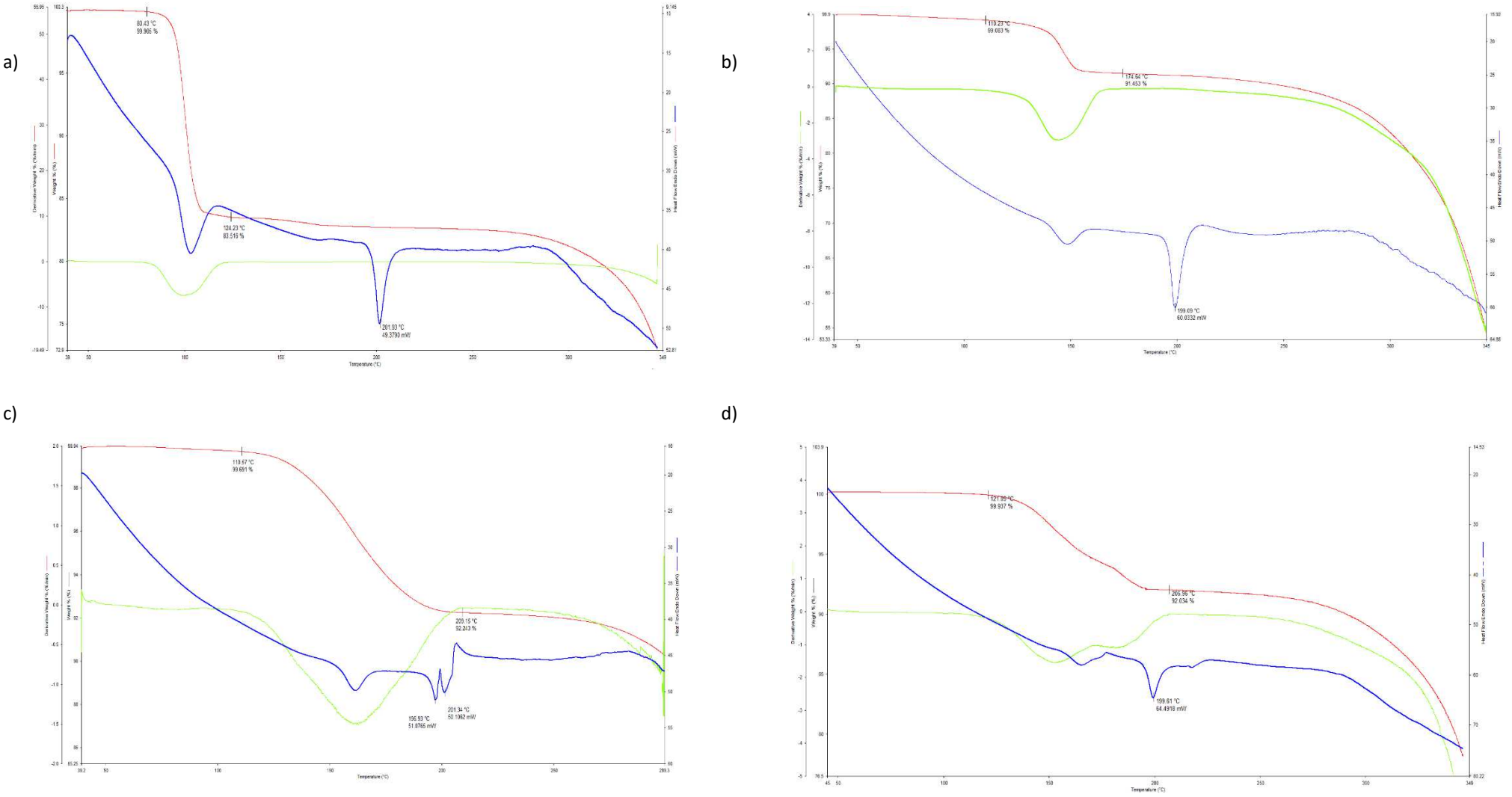


Figure 8 Overlaid DSC (blue, endo down), TG (red) and DTG (green) curves for (a) 2**H**·3(PYR), (b) 2**H**·2MP, (c) 2**H**·3MP and (d) 2**H**·4MP.

Table 5 Thermal properties of the four pyridyl complexes with **H**.

Complex	T_{on}[a] /°C	T_p[b] /°C	Measured mass loss /%	Expected mass loss /%
2**H**·3(PYR)[c]	[c]	201.9	16.4[c]	15.5 (H:G 2:3) and 19.6 (H:G 1:2)
2**H**·2MP	110.2	199.1	7.6	6.7
2**H**·3MP	110.6	201.3	7.4	6.7
2**H**·4MP	121.1	199.6	7.9	6.7

[a]The onset temperature of the guest release event.

[b]The temperature at which the host melt was most rapid.

[c]This complex was unstable at ambient conditions.

These thermal curves demonstrate that the experimentally obtained mass losses and those expected for the MP-containing complexes are in reasonable agreement (7.6% vs 6.7% (2**H**·2MP), 7.4% vs 6.7% (2**H**·3MP) and 7.9% vs 6.7% (2**H**·4MP)) (Table 5). However, as noted in the SCXRD discussion where the PYR complex was shown to have a H:G ratio of 1:2 while NMR suggested 2:3, this thermal experiment confirmed that the PYR complex was unstable at ambient conditions. It is plausible that during sample preparation for this experiment, as was the case for the ^{1}H-NMR experiment, some guest escaped from the crystals of its 1:2 complex, and only 16.4% mass loss was measured (alluding to a H:G ratio consistent with 2:3) rather than 19.6% (which is required for a 1:2 H:G ratio). T_{on} could, thus, also not be determined for this complex, nor is it possible to comment on the nature of the guest release event, whether in a single step or not. However, both PYR (Figure 8a) and 2MP (Figure 8b) were released from the cavities of the complex over a broad temperature range, the latter in a single step. In both cases, guest release concluded prior to the host melt event at approximately 200 °C. 3MP (Figure 8c) and 4MP (Figure 8d), on the other hand, while also escaping over a very broad temperature range, appeared to continue escaping from the complex even during the melting of the host species, with one release step event evident in the former instance and two in the latter. Finally, the relative thermal stabilities of these complexes, through a consideration of T_{on}, may thus be written as in the order 2**H**·4MP (121.1 °C) > 2**H**·3MP (110.6 °C) ≈ 2**H**·2MP (110.2 °C) >> 2**H**·3(PYR) (unstable at ambient conditions). These results concur exactly with the guest accommodation type observed in the SCXRD experiments, in discrete cavities in the case of the MPs, and in channels in the complex with PYR (which supports facile guest escape).

4. Conclusions

Here, **H** was shown to have the ability to form complexes with each of PYR, 2MP, 3MP and 4MP. Equimolar guest competition experiments demonstrated that PYR, 3MP and 4MP were favoured by **H** and that this preferential behaviour was highly dependent on the number and nature of the other guest solvents present; 2MP, however, was consistently disfavoured. The binary guest solution experiments revealed that each of the 50:50, 60:40 and 80:20 PYR/2MP, 20:80 and 40:60 3MP/PYR, and 50:50, 60:40 and 80:20 PYR/4MP mixtures may be separated effectively using **H** as the host species since all of these experiments furnished overwhelming K values, even infinite in many instances. PYR remained the favoured guest in these solutions. The SCXRD experiments illustrated that the host packing arrangements in the three MP-containing complexes were isostructural, while this packing was unique in **H**·2(PYR). Moreover, PYR was located in endless undulating channels parallel to the b-axis, while the MPs were all accommodated in discrete cavities. The enhanced affinity of **H** for PYR was ascribed to the fact that this guest alone engaged in a non-classical hydrogen bond with **H**, this type of interaction being absent in the MP-containing complexes. Moreover, PYR also interacted with **H** by means of three C–H···π close contacts, which numbered fewer or were absent in the remaining complexes. Thermal analysis demonstrated that the complex with PYR was notably less stable than those with the MPs, possibly owing to PYR being located in channels, whilst the MPs, in their more stable inclusion crystals, were accommodated in isolated voids.

Supplementary information

The crystal structures of **H**·2(PYR), **H**·0.5(2MP), **H**·0.5(3MP) and **H**·0.5(4MP) were deposited at the Cambridge Crystallographic Data Centre (CCDC), and their deposition numbers are 2536897, 2536898, 2536899 and

2536903652, respectively. These data are freely accessible at www.ccdc.cam.ac.uk/structures/. Applicable ^{1}H-NMR spectra may also be found in this section.

Author contributions

B.B.: conceptualization; methodology; funding acquisition; project administration; resources; supervision; visualization; writing the original draft. M.R.C.: data curation; formal analysis; provision of various figures; assistance with writing the original draft; resources; visualization. J.A.V.: investigation; methodology; validation; compilation of all results.

Conflict of interest

There are no conflicts of interest to declare.

Acknowledgements

Financial support is acknowledged from the Nelson Mandela University and the National Research Foundation (NRF) of South Africa. M.R.C. thanks the University of Cape Town for access to research facilities.

References

(1) Ramsay, W. On Picoline and Its Derivatives. Lond. Edinb. Dublin *Philos. Mag. J. Sci.* **1876**, *2 (11)*, 269–281.

(2) Anderson, T. On the Constitution and Properties of Picoline, a New Organic Base from Coal-Tar. *Trans. R. Soc. Edinburgh* **1849**, *16*, 123–136. https://doi.org/10.1017/S0080456800024984

(3) Tschitschibabin, A. E. Über Kondensation der Aldehyde mit Ammoniak zu Pyridinbasen. *J. Prakt. Chem.* **1924**, *107 (1–4)*, 122–128.

(4) Shimizu, S.; Watanabe, N.; Kataoka, T.; Shoji, T.; Abe, N.; Morishita, S.; Ichimura, H. Pyridine and Pyridine Derivatives. In Ullmann's Encyclopedia of Industrial Chemistry; Wiley, 2000. https://doi.org/10.1002/14356007.a22_399

(5) Pala-Rosas, I.; Contreras, J. L.; Salmones, J.; López-Medina, R.; Angeles-Beltrán, D.; Zeifert, B.; Navarrete-Bolaños, J.; González-Hernández, N. N. Effects of the Acidic and Textural Properties of Y-Type Zeolites on the Synthesis of Pyridine and 3-Picoline from Acrolein and Ammonia. *Catalysts* **2023**, *13 (4)*. https://doi.org/10.3390/catal13040652

(6) Jiang, F.; Huang, J. J.; Xiao, W. Y.; Xiao, G. M.; Li, H. Y. Synthesis of Picolines over Metal Modified HZSM-5 Catalyst. *Asian J. Chem.* **2015**, *27 (7)*, 2415–2419. https://doi.org/10.14233/ajchem.2015.17883

(7) Calvin, J. R.; Davis, R. D.; McAteer, C. H. Mechanistic Investigation of the Catalyzed Vapor-Phase Formation of Pyridine and Quinoline Bases Using $^{13}CH_2O$, $^{13}CH_3OH$, and Deuterium-Labeled Aldehydes. *Appl. Catal. A Gen.* **2005**, *285 (1–2)*, 1–23. https://doi.org/10.1016/j.apcata.2004.10.021

(8) Shimizu, S.; Abe, N.; Iguchi', A.; Dohba, M.; Sato, H.; Hirose, K.-I. Synthesis of Pyridine Bases on Zeolite Catalyst. *Microporous Mesoporous. Mater.* **1998**, *21 (4–6)*, 447–451.

(9) Scriven, E. F. V.; Murugan, R. Pyridine and Pyridine Derivatives. In Kirk-Othmer Encyclopedia of Chemical Technology; John Wiley & Sons, Inc: Hoboken, NJ, 2005; Vol. 20.

(10) World Health Organization. Some Industrial Chemicals; IARC; Distributed by IARC Press and by the World Health Organization Distribution and Sales, 2000; Vol. 77.

(11) Higashio, Y.; Shoji, T. Heterocyclic Compounds Such as Pyrrole, Pyridines, Pyrrolidine, Piperidine, Indole, Imidazol and Pyrazines. *Appl. Catal. A Gen.* **2004**, *260 (2)*, 251–259. https://doi.org/10.1016/S0926-860X(03)00197-2

(12) Shishido, T.; Song, Z.; Kadowaki, E.; Wang, Y.; Takehira, K. Vapor-Phase Oxidation of 3-Picoline to Nicotinic Acid over $Cr_{1-x}Al_xVO_4$ Catalysts. *Appl. Catal. A Gen.* **2003**, *239 (1–2)*, 287–296.

(13) Jermakowicz-Bartkowiak, D.; Kolarz, B. N. Poly(4-Vinylpyridine) Resins towards Perrhenate Sorption and Desorption. *React. Funct. Polym.* **2011**, *71 (2)*, 95–103. https://doi.org/10.1016/j.reactfunctpolym.2010.11.023

(14) Duprat, F.; Gau, G. Reactive Distillation of Pyridine Mixtures with an Organic Acid. II. Parametric Sensitivity and Optimization of the Process. *Canadian J. Chem. Eng.* **1991**, *69 (6)*, 1327–1335.

(15) Zhu, X.; Yan, M.; Zhang, Y.; Chen, J.; Zhu, H.; Chi, Y.; Yu, Y.; Zhou, J. Selective Adsorption and Separation of Pyridine and Picoline Using Hybrid[3]Arene-Based Nonporous Adaptive Crystals. *Mater. Chem. Front.* **2026**, *10 (14)*, 2302–2309. https://doi.org/10.1039/d6qm00116e

(16) Franke, M. B.; Schuur, B. Dissociation Extraction: Theoretical Foundations and Applications. *Sep. Purif. Technol.* **2024**, *350*, 127888. https://doi.org/10.1016/j.seppur.2024.127888

(17) Gaikar, V. G.; Sharma, M. M. Separations Through Reactions and Other Novel Strategies. *Sep. Purif. Rev.* **1989**, *18 (2)*, 111–176. https://doi.org/10.1080/03602548908050922

(18) Puttreddy, R.; Beyeh, N. K.; Rissanen, K. Inclusion Complexes of C Ethyl-2-Methylresorcinarene and Pyridine N-Oxides: Breaking the C-I···-O-N+ Halogen Bond by Host-Guest Complexation. *CrystEngComm* **2016**, 18 (5), *793–799*. https://doi.org/10.1039/c5ce02354h

(19) Zhou, H. Y.; Chen, C. F. Adsorptive Separation of Picoline Isomers by Adaptive Calix[3]Acridan Crystals. *Chem. Commun.* **2022**, *58 (27)*, 4356–4359. https://doi.org/10.1039/d2cc00943a

(20) Caira, M. R.; Le Roex, T.; Nassimbeni, L. R. Selective Enclathration of Picoline Isomers by a Resorcinarene Host. *CrystEngComm* **2006**, *8 (3)*, 275–280. https://doi.org/10.1039/b601560c

(21) Zeng, Y.; Liang, C.; Lu, X.; Zhao, L.; Wu, F.; Hou, T.; Zhao, A.; Lv, M.; Tao, Z.; Li, Q. Perfect Separation of Pyridine and 3-Methylpyridine by Cucurbit[6]Uril. *Chin. Chem. Lett.* **2025**, *36 (9)*, 110807. https://doi.org/10.1016/j.cclet.2024.110807

(22) Bourne, S. A.; Corin, K. C.; Nassimbeni, L. R.; Toda, F. Selective Enclathration of Picolines. *Cryst. Growth Des.* **2005**, *5 (1)*, 379–382. https://doi.org/10.1021/cg049848f

(23) Bawa, H.; Su, H.; De Doncker, S.; Bourne, S. A.; Nassimbeni, L. R. Selectivity of Picoline by Enclathration: Structure and Kinetics of Decomposition. *Cryst. Growth Des.* **2024**, *24 (20)*, 8550–8556. https://doi.org/10.1021/acs.cgd.4c01061

(24) Barton, B.; Caira, M. R.; Vorgers, J.; Hosten, E. C. Investigation of the Hydrogen Bonded Host· · · guest and Guest· · · guest Interactions Present in Complexes of a Polyaromatic Wheel-and-Axle Host Compound with Dioxane, Morpholine, Piperidine and Pyridine. *J. Incl. Phenom. Macrocycl. Chem.* **2023**, *104*, 15–24. https://doi.org/10.1007/s10847-023-01210-4

(25) Barton, B.; Vorgers, J. A.; Hosten, E. C. Crystallization Experiments of the Wheel-and-Axle Host Compound, 1,4-Phenylene-Bis(Di-p-Tolylmethanol), from Pyridine and Methylpyridine Mixtures. *J. Incl. Phenom. Macrocycl. Chem.* 2024, *104 (9–10)*, 473–485. https://doi.org/10.1007/s10847-024-01248-y

(26) Barton, B.; Vorgers, J. A.; Hosten, E. C. Exploring the Host Compound Dynamics of 1,4-Phenylene-Bis(Di-*p*-Fluorophenylmethanol) in Mixed Pyridines. *J. Incl. Phenom. Macrocycl. Chem.* **2025**, *105*, 35–48. https://doi.org/10.1007/s10847-024-01264-y

(27) Barton, B.; de Jager, L.; Hosten, E. C. Host Proficiency of *N*,*N'*-Bis(9-Phenyl-9-Thioxanthenyl)Ethylenediamine for Pyridine and the Methylpyridine Guests–a Competition Study. *Supramol. Chem.* **2018**, *30 (1)*, 61–71. https://doi.org/10.1080/10610278.2017.1361037

(28) Barton, B.; Caira, M. R.; Trollip, D. B.; Hosten, E. C. The Behaviour of Tricyclic Fused Host Systems Comprising Seven-Membered B-Rings in Mixed Pyridines. *CrystEngComm* **2023**, *25 (45)*, 6317–6328. https://doi.org/10.1039/d3ce00811h

(29) Groenewaldt, J. L.; Barton, B.; Hosten, E. C. The Selectivity Behaviour of 9,9'-Bifluorenyl-9,9'-Diol as a Host Compound for Highly Efficient Separations of Mixed Pyridines. *CrystEngComm* **2025**, *27 (24)*, 4176–4188. https://doi.org/10.1039/d5ce00432b

(30) Barton, B.; Caira, M. R.; Senekal, U.; Hosten, E. C. Complementary Host Behaviour of Three Anthracenyl-Derived Roof-Shaped Compounds in Mixed Pyridines. *CrystEngComm* **2023**, *25 (12)*, 1740–1754. https://doi.org/10.1039/d3ce00080j

(31) Recchia, D. L.; Barton, B.; Hosten, E. C. Exploring Supramolecular Chemistry as an Innovative Strategy for Pyridine Guest Separations When Employing a TADDOL Derivative as the Host Compound. *Cryst. Growth Des.* **2024**, *24 (15)*, 6438–6449. https://doi.org/10.1021/acs.cgd.4c00717

(32) Bruker AXS Inc. APEX3 (Version 2019.1-0). Bruker AXS Inc.: Madison, Wisconsin, USA.

(33) Krause, L.; Herbst-Irmer, R.; Sheldrick, G. M.; Stalke, D. Comparison of Silver and Molybdenum Microfocus X-Ray Sources for Single-Crystal Structure Determination. *J. Appl. Crystallogr.* **2015**, *48 (1)*, 3–10. https://doi.org/10.1107/S1600576714022985

(34) Sheldrick, G. M. A Short History of SHELX. *Acta Crystallogr. A* **2008**, *64 (1)*, 112–122. https://doi.org/10.1107/S0108767307043930

(35) Barbour, L. J. X-Seed 4: Updates to a Program for Small-Molecule Supramolecular Crystallography. *J. Appl. Crystallogr.* **2020**, *53*, 1141–1146. https://doi.org/10.1107/S1600576720007438

(36) Trollip, D. B. Fused Tricyclic Systems as Host Compounds for the Potential Separation of Isomers and Related Compounds through Supramolecular Chemistry Protocols, Nelson Mandela University, 2026.

(37) Pivovar, A. M.; Holman, K. T.; Ward, M. D. Shape-Selective Separation of Molecular Isomers with Tunable Hydrogen-Bonded Host Frameworks. *Chem. Mater.* **2001**, *13 (9)*, 3018–3031. https://doi.org/10.1021/cm0104452

(38) Nassimbeni, L. R.; Sykes, N. M. Inclusion Compounds: Structure, Kinetics and Selectivity. *Crystallogr. Rev.* **2022**, 28 (2–3), 70–96. https://doi.org/10.1080/0889311X.2022.2067849

(39) Sykes, N. M.; Su, H.; Weber, E.; Bourne, S. A.; Nassimbeni, L. R. Selective Enclathration of Methyl-And Dimethylpiperidines by Fluorenol Hosts. *Cryst. Growth Des.* **2017**, *17 (2)*, 819–826. https://doi.org/10.1021/acs.cgd.6b01661

(40) Macrae, C.; Sovago, I.; Cottrell, S.; Galek, P.; McCabe, P.; Padcock, E.; Platings, M.; Shields, G.; Stevens, J.; Towler, M.; Wood, P. Mercury 4.0: From Visualization to Analysis. Design and Prediction. *J. Appl. Crystallogr.* **2020**, *53*, 226–235.

Supplementary Files

This is a list of supplementary files associated with this preprint. Click to download.

- SUPPLEMENTARYINFORMATION.docx